JUPITER BURST OBSERVATION WITH LOFAR/ITS

A. Nigl[*], J. Kuijpers[*], H. Falcke[†*], P. Zarka[‡], and L. Bähren[†]

Abstract

Io-induced Jupiter emission lies mainly in the frequency range from about 2 to 40 MHz [Zarka et al., 2001], which happens to coincide with the frequency band of the Low-Frequency Radio Array Initial Test Station (LOFAR/ITS). ITS is capable of measuring the radio signal with high time and frequency resolution, which makes it well-suited for the study of Jovian decametric emission (DAM). We present the first simultaneous Io-DAM observations of Jupiter at about 700 km distance between two instruments, LOFAR/ITS and the Nançay Decametric Array (NDA). We have detected emission from Jupiter during snapshots of a few seconds and identified detailed features in dynamic spectra taken with both instruments. This will be the basis for VLBI-like correlation of both waveforms. This article presents first and preliminary Jupiter observations with ITS. We analyze Faraday rotation, which is measured with linearly polarized antennas. We observe frequency modulation over a broad spectral range and demonstrate that the effect comes mainly from the Earth's ionosphere. This article presents first observations and discusses frequency modulated Faraday rotation.

1 Introduction

Jupiter's radio emission was discovered in 1955 by B.F. Burke and K.L. Franklin at a frequency of 22.2 MHz. Jupiter's radio emission takes place below 40 MHz, limited by the maximum electron gyrofrequency at the surface. The lower limit for ground-based observations is set by the plasmafrequency of the Earth's ionosphere between 5 and 10 MHz (see Fig. 1, [Zarka, 2004]). This emission band covers exactly the frequency range of LOFAR's Initial Test Station (ITS). ITS is an interferometer of simple dipole antennas located in the Dutch province Drenthe close to the small village Exloo. Triggered by the Nançay Decametric Array (NDA) close to Paris, we took simultaneous data sets during periods of Jupiter burst emission detected on Earth. Since 1964, Jupiter's decametric

[*] *Department of Astrophysics (IMAPP), Radboud University Nijmegen, The Netherlands*
[†] *ASTRON, Dwingeloo, The Netherlands*
[‡] *Observatoire de Paris, LESIA, UMR CNRS 8109, 92195 Meudon, France*

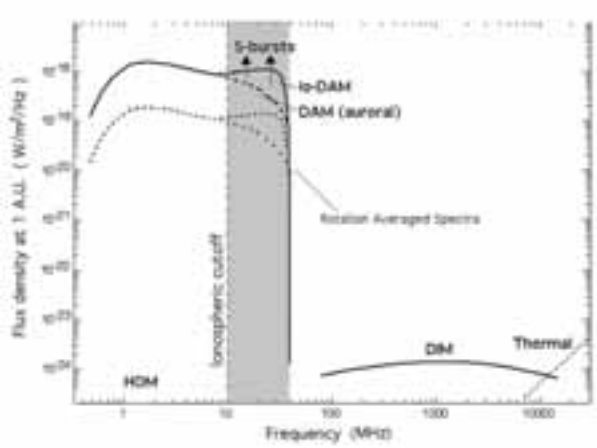

Figure 1: Spectra of Jovian radio components. Decametric emission as a superposition of auroral DAM (dashed) down to hectometric emission (HOM) and Io-DAM with impulsive bursts (S-bursts). Decimetric emission (DIM) is standing for synchrotron emission from Jupiter's radiation belts. [Zarka, 2004]

emission (DAM) has been known to be modulated by the position of Io [Bigg, 1964]. Io is the innermost Galilean satellite at an average radial distance of 5.95 R_J and a period of 1.769 days. This moon is the volcanically most active body in our solar system and thus the source of much of the heavy ion plasma filling Jupiter's magnetosphere [Carr, 1983]. Io's volcanos eject about one ton per second of mainly sulfur compounds such as SO_2 in Jupiter's magnetosphere. The expelled plasma becomes ionized and fills a torus-shaped cloud (r = 5 to 7 R_J) in which the electron density can reach 2000 cm^{-3}. This cloud is called the Io Plasma Torus (IPT) [Thomas, 2004]. Because of the relative motion between Io and the magnetosphere a large net electromotive force (400 kV) develops, which produces a current of about 10 million Ampères in the so-called Io Flux Tube (IFT) [Neubauer, 1980]. Electrons accelerated along the flux tube produce strong decametric emission at the reflection point above Jupiter's magnetosphere. The emission mechanism of Jupiter's DAM is believed to be the cyclotron maser instability, which will be explained in the next Section.
In Section 3 the two instruments ITS and NDA are described, with which the Io-DAM observations presented in Section 4 were obtained. In Section 5, we demonstrate that the observed frequency modulation in the ITS signal can be understood as Faraday rotation, and we discuss the origin of the rotation measure.

2 Emission Mechanism

The motion of Io through Jupiter's magnetosphere creates a wake of magneto–hydrodynamic (MHD) pertubations. It is expected that in particular Alfvén waves develop a parallel electric field, which accelerates electrons from the surrounding Io plasma along Jupiter's field lines towards the planet. For the down-going electrons the beam distribution is itself not favorable for radio wave generation. However, at the reflection point, partial mirroring takes place, and a loss-cone distribution is formed. The reflected electron distribution is

unstable to the direct production of electromagnetic waves through the cyclotron maser instability [Zarka, 1998] at a multiple of the local non-relativistic cyclotron frequency:

$$\nu_{ce} \;=\; \frac{e\,B}{2\pi\,m_e} \;\text{ thus }\; \nu_{ce}\;(\text{MHz}) = 2.8 \times B\,(\text{G})\,, \tag{1}$$

where e_c is the electron charge, m_e the electron mass and B the magnetic flux density at the emission point. The emission is beamed into a thin hollow cone with its axis parallel to the magnetic field lines originating close to the Jovian magnetic poles, a half-angle of 60-90° relative to the local magnetic field direction and a cone wall thickness of a few degrees [Queinnec and Zarka, 1998]. The emission can be detected on Earth, when the line of sight of the observer coincides with the wall of the hollow cone. The emission can arrive in short and narrow bursts, so-called S-bursts [Zarka et al., 1996].

3 Radiotelescopes

ITS

LOFAR's initial test station (www.lofar.org) is located at the future core site of LOFAR and consists of 60 inverted-V-shaped dipoles distributed over five spiral arms. Each dipole's signal is amplified in an LNA (low-noise amplifier), filtered in frequency and then digitized. High performance Analog-Digital Converters (ADCs) with a dynamic range of 12 bits supply a rate of 80 million samples per second, which translates to a time resolution of 12.5 ns and a data rate of $\sim$ 150 MB per second and dipole. Because of the crossed and inverted-V-shape design of the antenna dipoles, the whole sky can be measured simultaneously with a primary beam of 90° centered on the zenith. With real-time or off-line beam-forming the array can be pointed at any source in the sky.

NDA

The Nançay Decametric Array (www.obs-nancay.fr) is an interferometer consisting of 144 antennas. Each antenna consists of 8 conducting wires wound in spirals on a conical surface. Half of the antennas is left- and half is right-handed wound to measure circularly polarized radio waves. A full description of the array can be found elsewhere [Boischot et al., 1980].

4 Observations

On June 22, 2004, simultaneous Jupiter snapshots of 6.7 s (1 GB) have been recorded with LOFAR/ITS and NDA. Here, we focus on one of the observations at 15:37:34 UTC $\pm$ 3.5 s. The geometry of Earth, Jupiter and Io is pictured in Fig. 2 [LEFT]. At the time of the observation, Io was on the west side of Jupiter as seen from Earth at a phase of $\phi_{\text{Io}} = 91.40°$. Jupiter's magnetic axis was tilted in Io's direction, which translates to a

Jupiter central meridian longitude (CML) of CML = 131.02° (see Fig. 2 [LEFT]). Fig. 2 [RIGHT] shows the orientation of the Io plasma torus with respect to the rotational and magnetic axes.

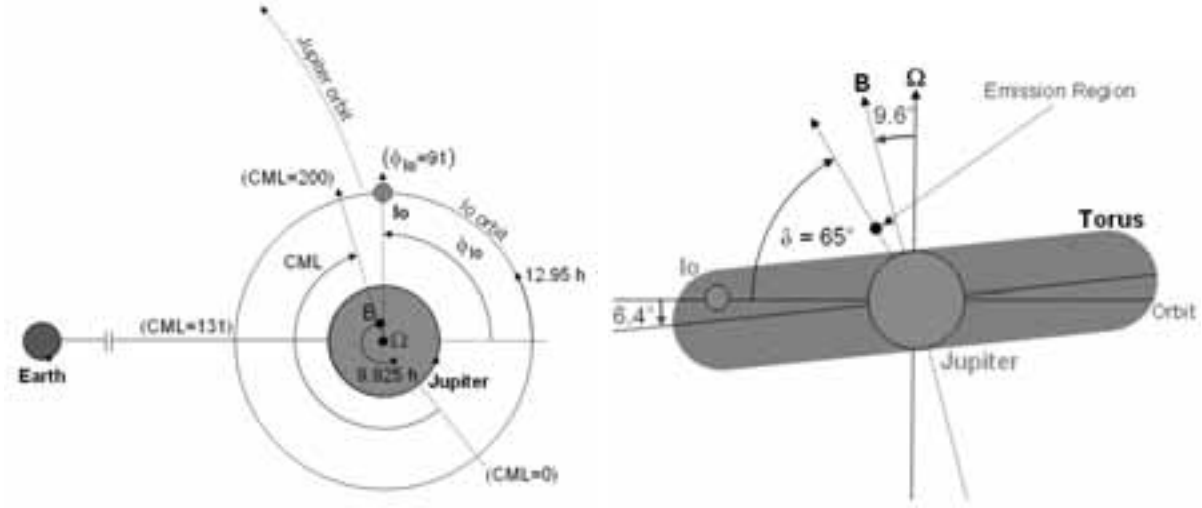

Figure 2: Jupiter Io configuration on June 22, 2004 at 15:37:34 UTC as seen from Earth, [LEFT] showing Jupiter CML and Io phase at the time of observation and [RIGHT] the Jupiter Io configuration face on. The reference for the Jupiter system III (1965) is the central meridian longitude (CML) at 200°, which connects the rotational and magnetic axes [Dessler, 1983].

Both telescopes recorded the full waveform at the same time. To combine the antennas of ITS, so-called beam-forming is used. For beam-forming the antenna signals are transformed to the Fourier domain by FFT (see spectrum in Fig. 4 [LEFT]). In the frequency domain, the interesting bands are selected and the phase delays are applied corresponding to the light travel time for the signal between each antenna and a reference antenna. The resulting beam-spectra are used for the dynamic spectrum, which is displayed in Fig. 3 [LEFT]. For comparison of the simultaneous data, the dynamic spectra of ITS and NDA are plotted in Fig. 3 [RIGHT].

Since the radiation emitted from Io's interaction with Jupiter is strongly elliptically polarized [Zarka, 1998], NDA was measuring the emission with all 72 right-handed wound antennas and thus sensitive to the corresponding part of circular polarization. ITS on the other hand observed with 48 aligned dipoles and thus measured one linear component of the electric field.

A spectrum calculated for the whole snapshot of 6.7 seconds is plotted in Fig. 4 [RIGHT] (black line). The spectrum shows a quasi-periodic feature in frequency with alternating bands of maxima/minima and variable bandwidth. This frequency feature can also be seen in the dynamic spectra as horizontal bands in Fig. 3 [LEFT]. This effect will be explained as Faraday rotation in the next Section.

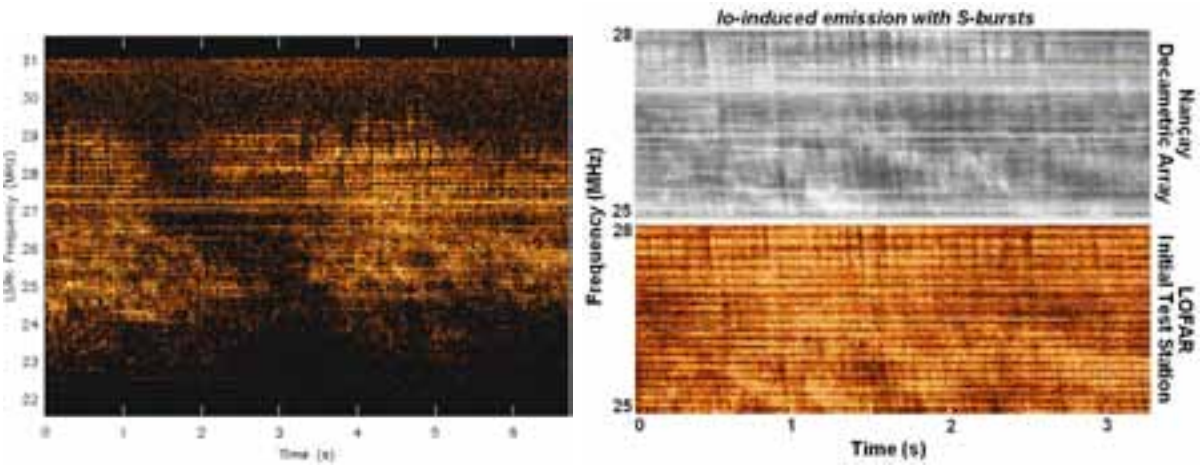

Figure 3: [LEFT] This figure shows a dynamic spectrum of an ITS observation from June 22, 2004 at 15:37:34 UTC ±3.5 s beamed in the direction of Jupiter with 48 dipole antennas. [RIGHT] This figure compares three seconds (15:37:35 to 15:37:38 UTC) of the dynamic spectra for the Jupiter-Io burst from June 22, 2004 observed with the Nançay Decametric Array (bottom) and LOFAR Initial Test Station (top) from 25 to 28 MHz.

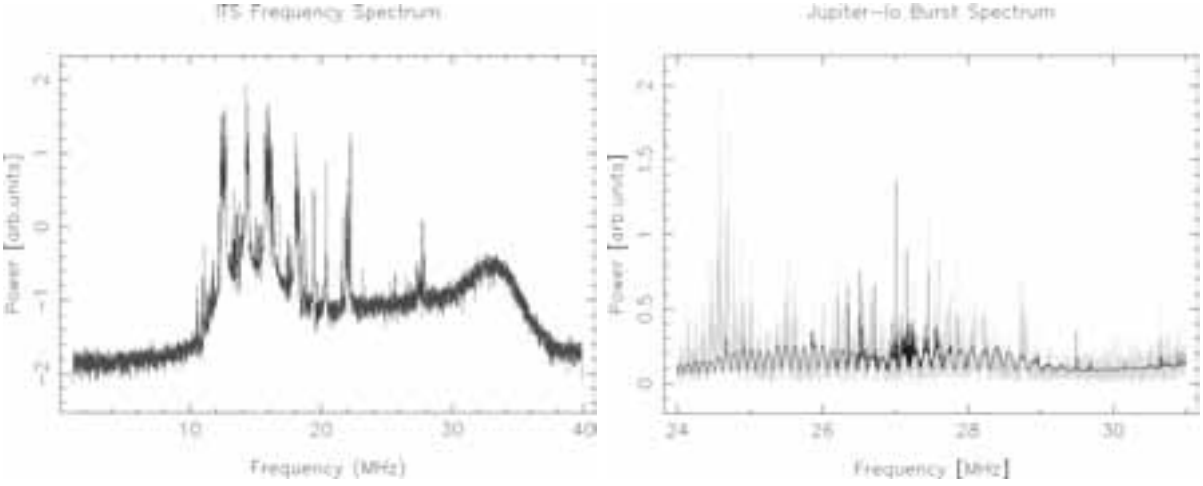

Figure 4: [LEFT] Spectrum of LOFAR's Initial Test Station (ITS). The interesting part in Jupiter observations is the band between 22 and 30 MHz; below 22 MHz is strong RFI and above 30 MHz a non-linear bandpass characteristic. [RIGHT] The figure shows a Jupiter-beam frequency spectrum from 25 to 31 MHz with about one millisecond integration time (GREY) overlayed with another Jupiter-beam frequency spectrum calculated for 6.7 seconds of maximum continuous observation time (BLACK).

5 Faraday Rotation

5.1 Theory

On its way from Jupiter to Earth, the received electromagnetic radiation is affected by the intervening magnetoplasma. Any high-frequency signal can be split up in two eigen modes, namely X-mode and O-mode. Because of the relatively small magnetic field, the

quasi-longitudinal approximation (QL) applies except in a very narrow range of angles perpendicular to the local magnetic field direction [Pacholczyk, 1970]. In QL propagation both X- and O-mode are oppositely circularly polarized. Since both modes propagate at different phase velocities an initial linearly polarized signal remains linearly polarized after transit through the interplanetary plasma, but with different orientation. This effect is called Faraday Rotation, also called the Magneto-Optic Effect, which was discovered by Michael Faraday in 1845. The Faraday Rotation angle χ_F over which the plane of polarization rotates is given by:

$$\chi_F = \int \frac{\omega}{2c} (n_o - n_x)\, ds = \int \frac{1}{2} \frac{\omega_0^2 \omega_G}{c\,\omega^2} ds = RM \frac{c^2}{\nu^2}, \tag{2}$$

where $\omega = 2\pi\nu$ is the frequency of the wave, n_o and n_x represent the index of refraction for the ordinary and extraordinary wave mode and s stands for the path length along the line of sight. We have used:

$$n_{o/x} = \sqrt{1 - \frac{\omega_0^2}{\omega\,(\omega \pm \omega_G)}}, \tag{3}$$

where ω_0 is the plasma frequency and $\omega_G = 2\pi\nu_{ce}$ (Eq. 1) the Larmor (or non-relativistic cyclotron) frequency, and we have assumed that the frequency of the wave is much greater than the plasma and Larmor frequency ($\omega >> \omega_0, \omega_G$).
Thus, the rotation measure RM is defined as:

$$RM = \frac{e^3}{8\pi^2\, m_e^2\, c^3\, \epsilon_0} \int n_e\, \vec{B} \cdot \vec{ds}. \tag{4}$$

5.2 Calculation of Faraday rotation

The electromagnetic radiation is affected by Faraday Rotation in essentially four regions with different densities: (1) Jupiter's magnetosphere, (2) the Io torus, (3) the interplanetary medium (IPM), and (4) the Earth's ionosphere during daytime. We estimate the various contributions to the Faraday rotation with average values for the magnetic flux density B, the electron density n_e and path-length s for the different regions:
(1) For Jupiter's magnetosphere we take an extension of about 30 Jupiter radii, an average magnetic field strength of $B_J = 0.14$ G and a mean electron density of $n_J = 5$ cm^{-3} and get a rotation measure of $RM_J = 4 \times 10^{-2}$ rad/m^2.
(2) For the Io torus we use a radius of one Jupiter radius, an average magnetic field strength of $B_J = 0.02$ G and a mean electron density of $n_J = 665$ cm^{-3}, which results in a rotation measure of $RM_J = 9 \times 10^{-3}$ rad/m^2.
(3) The interplanetary medium in between Jupiter and Earth: $s_{IPM} = 5.686$ AU, an average magnetic field strength of $B_{IPM} = 5 \times 10^{-5}$ G and an electron density of $n_{IPM} = 5$ cm^{-3} (solar wind), resulting in a rotation measure of $RM_J = 6 \times 10^{-3}$ rad/m^2.
(4) At the Earth, the magnetosphere is small compared to Jupiter's, but the high electron density of the ionosphere with an extension of 500 km, an average value of $n_E = 5 \times 10^5$ cm^{-3} and an average magnetic field strength of $B_E = 2 \times 10^{-1}$ G give a rotation

measure of $RM = 2$ rad/m^2, which is by far the largest contribution.

According to our theoretical estimate, 96% of the Faraday rotation is contributed by the Earth's ionosphere and only 4% by Jupiter's magnetosphere. This is in nice agreement with Warwick and Dulk [1964], where at least 90% of the Faraday rotation occurs in the terrestrial ionosphere and 10% can be attributed to plasma inside Jupiter's magnetosphere.

5.3 Comparision to observations

To derive a first approximation for the Faraday rotation from the measured data, we use the change in frequency between two minima. For neighbouring frequencies, the differential Faraday rotation reads:

$$RM = \frac{\pi}{2\,\Delta\nu\,c^2}\,\nu^3, \tag{5}$$

where $\Delta\nu$ is the difference in frequency for one complete rotation of the plane of polarization at frequency ν. At $\nu = 27$ MHz the difference in frequency for two succesive minima (one full rotation) is $\Delta\nu = 150$ kHz. Inserting these numbers in the eq. 5 results in a rotation measure of $RM = 2.3$ rad/m^2.
As a next step the spectrum has to be cleaned from Radio Frequency Interference (RFI), so that a curve can be fitted to all minima. The fit delivers an accurate number on the power law (slope) of the observed frequency feature (see Fig. 5 [LEFT]). To confirm the importance of Faraday rotation, we fit the function $log|\Delta\nu| = x \cdot log|\nu| + log|k|$ to the minima of the spectrum in Fig. 5 [RIGHT]. The best fit is for $x = 3.05$ and $k = RM \cdot c^2 = 4.98 \times 10^{17}$ s^{-2}. The obtained slope for the differential Faraday rotation is according Eq. 5 close to a cubic power law. The value for the rotation measure results in $RM = 2.77$ rad/m^2. This confirms Faraday rotation as the origin of the observed frequency modulation.

6 Conclusion

Using the prototype of the new generation radio telescope LOFAR, Io-induced Jupiter radio emission and S-bursts were detected. The prototype ITS consists of 60 simple dipoles, that measure the whole sky at the same time, including strong radio frequency interference (RFI). With the resulting high noise level it turns out not to be possible to observe Jupiter's emission in one single dipole. Thus, phasing the antennas by so-called beam-forming in the direction of Jupiter improved the signal-to-noise ratio, so that the emission became visible. The dynamic spectra obtained in this way show good agreement between ITS and NDA (see Fig. 3 [RIGHT]).
Additionally, there are horizontal bands in the dynamic spectrum from ITS only, which were clearly identified by calculating a spectrum over the whole observation of 6.7 seconds

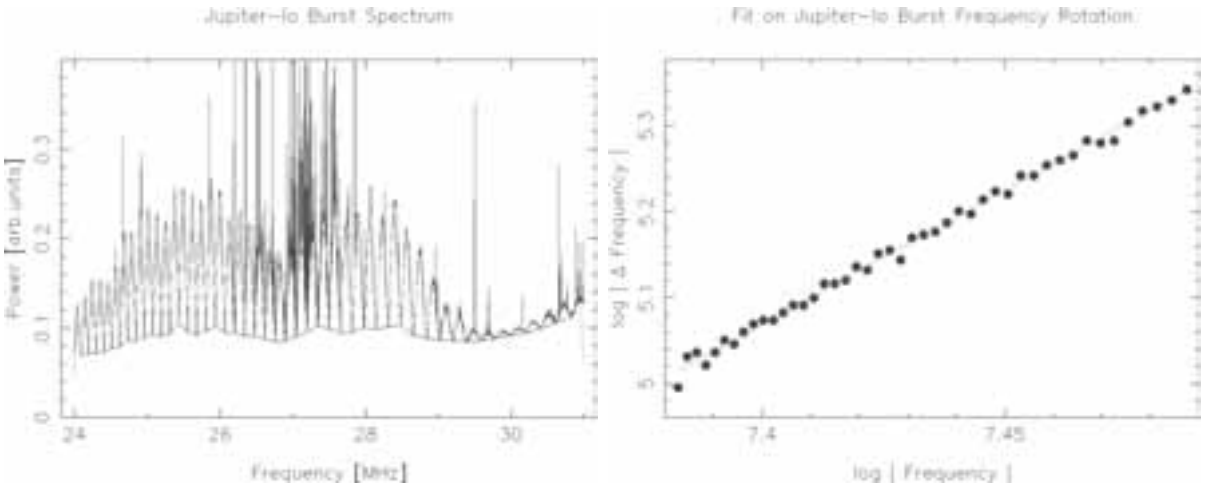

Figure 5: [LEFT] The plot shows the Jupiter-beam frequency spectrum from 24 to 31 MHz including RFI overlayed with a block-averaged spectrum and a envelope to the minima. [RIGHT] In this plot the change in frequency between the successive minima $log|\Delta\nu|$ is plotted as a function of frequency $log|\nu|$.

(see Fig. 4 [RIGHT]). Making a fit to the minima of this quasi-periodic feature, shows that the change in frequency agrees with the cubic power law of Faraday rotation. The resulting values for the fitted and calculated rotation measure of $RM = 2$ rad/m^2, $RM = 2.77$ rad/m^2 are in good agreement.
With its sensitivity and angular resolution, LOFAR will be perfectly suitable to study emission of planets like Jupiter at very low frequencies. Additionally, short-time structures in the signal, such as Jupiter's S-bursts can be studied with the high time and frequency resolution provided by the LOFAR hardware.
A positive correlation of the dynamic spectra in Fig. 3 indicates that a correlations of the pure waveforms from ITS and NDA (with a distance of about 700 km) is a reasonable next step. By correlation of the waveforms, we plan to identify the influence of the ionosphere on VLBI with LOFAR. If this method turns out to be feasible, it will be a strong argument to implement LOFAR stations at up to these distances from the array core, in order to reach a spatial resolution < 2" above 30 MHz. Such a resolution will provide the possibility to perform detailed Jupiter studies described in [Zarka, 2004].
Finally, with the new setup of ITS, having 30 crossed dipoles, polarization of the signal can be studied to a greater detail.

References

Bigg, E. K., Influence of the Satellite Io on Jupiter's Decametric Emission, in *Nature*, **203**, 1008-1010, 1964.

Boischot, A., C. Rosolen, M. G. Aubier, G. Daigne, F. Genova, Y. Leblanc, A. Lecacheux, J. de La Noe, and B. Moller-Pedersen, A new high-gain, broadband, steerable array to study Jovian decametric emission, *Icarus*, **43**, 399, 1980.

Burke, B. F., and Franklin, K. L., Observations of a Variable Radio Source Associated with the Planet Jupiter, *J. Geophys. Res.*, **60**, 213-217, 1955.

Carr, T. D., M. D. Desch, and J. K. Alexander, Phenomenology of magnetospheric radio emissions, in *Physics of the Jovian Magnetosphere,* edited by A. J. Dessler, *Cambridge University Press, New York*, 226–284, 1983.

Dessler, A. J., Coordinate systems, in *Physics of the Jovian magnetosphere*, edited by A. J. Dessler, *Cambridge Univ. Press, Cambridge*, 498, 1983.

Kaiser, M. L., P. Zarka, W. S. Kurth, G. B. Hospodarsky, and D. A. Gurnett, Cassini and Wind stereoscopic observations of Jovian non-thermal radio emissions: measurements of beamwidths, *J. Geophys. Res.*, **105**, 16053-16062, 2000.

Neubauer, F. M., Nonlinear standing Alfvén wave current systemat Io: Theory, *J. Geophys. Res.*, **85**, 1171, 1980.

Pacholczyk, A. G., Radio Astrophysics - Nonthermal Processes in Galactic and Extragalactic Sources, *W. H. Freeman*, 1970.

Queinnec, J., and P. Zarka, Io-Controlled Decameter Arcs and Io-Jupiter Interaction, *J. Geophys. Res.*, **103**, 26649-26666, 1998.

Thomas, N., F. Bagenal, T. W. Hill, and J. K. Wilson, The Io Neutral Clouds and Plasma Torus, in *Jupiter - The Planet, Satellites and Magnetosphere*, *Cambridge University Press, Cambridge, U. K.*, 561–591, 2004.

Warwick, J. W., and G. A. Dulk, Faraday rotation on decametric radio emission from Jupiter, *Science*, **145**, 380, 1964.

Zarka, P., Auroral radio emissions at the outer planets: observations and theories, *J. Geophys. Res.*, **103**, 20159-20194, 1998.

Zarka, P., Fast radio imaging of Jupiter's magnetosphere at low-frequencies with LOFAR, *Planet. Space Sci.*, **52**, 1455-1467, 2004.

Zarka, P., T. Farges, B. P. Ryabov, M. Abada-Simon, and L. Denis, A scenario for jovian S-bursts, *Geophys. Res. Lett.*, **23**, 125-128, 1996.

Zarka, P., J. Queinnec, and F. Crary, Low-frequency limit of Jovian radio emissions and implications on source locations and Io plasma wake, *Planet. Space Sci.*, **49**, 1137-1149, 2001.